Macromolecules

ARTICLE

pubs.acs.org/Macromolecules

Automatic Spray-LBL Machine Based on *in-Situ* QCM Monitoring

Nanae Fukao, Kyu-Hong Kyung, Kouji Fujimoto, and Seimei Shiratori*

Graduate School of Science and Technology, Keio University, 3-14-1, Hiyoshi, Kouhoku-ku, Yokohama 223-8522, Japan

ABSTRACT: Aqueous-based spray-layer-by-layer (spray-LBL) techniques have become an innovative, economic, and fast fabrication process, particularly in comparison to conventional LBL dipping techniques. The spray-LBL method has enhanced the growth of polyelectrolyte multilayer films using spray pressure. In this study, we have fabricated an automatic spray-LBL machine and have monitored the real-time growth of multilayer films using quartz crystal microbalance (QCM) techniques. We have discussed the process of multilayer thin film growth and the effect of spray pressure on film growth. We have fabricated polyelectrolyte multilayer films on gold, using poly(allylamine hydrochloride) (PAH) as the polycation and poly(acrylic acid) (PAA) as the polyanion. UV−vis spectroscopic data showed that visible light transmission was similar to that of bare slide glass. Fabrication using the automatic spray-LBL machine and real-time QCM monitoring allows the fabrication of optical quality thin films with precise thickness.

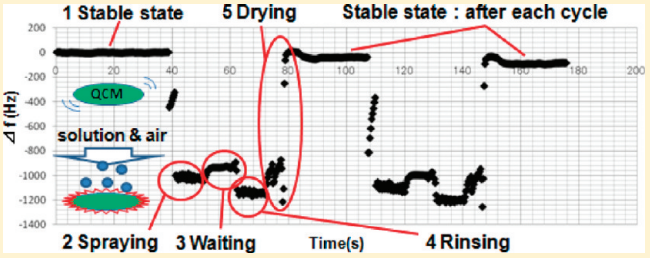

INTRODUCTION

Optical thin films can control the transmission and reflection of specific wavelengths of light and have numerous applications. They are used as visible optical antireflection films for glasses and windows and also to raise the photoelectric conversion efficiency of solar batteries.[1−3] Band-pass filters that selectively transmit monochromatic light are used in cameras and photocells, along with other increasing numbers of appications.[4,5] Eco-friendly films that selectively reflect near-infrared radiation have also been developed.[6] As such films do not transmit heat in the near-infrared region, the increase in indoor temperature can be suppressed by applying these films to windows. For all the above optical applications, the precise control of film thickness and reflective index is necessary. Consequently, vapor metal deposition on substrates is typically carried out under vacuum, which generally limits the fabrication of reproducible optical thin films to industrial processes. For other applications like windows which require film formation over a wide area, the production cost under vacuum conditions can be prohibitive, since large volume vacuum containers and considerable energy to achieve vacuum are required.

The layer-by-layer (LBL) self-assembly method appears promising for overcoming the above difficulties.[7−9] It is an easy, aqueous-based, eco-friendly method carried out under room temperature and at 1 atm and has been thoroughly explored by Gero Decher et al.[7] A disadvantage was that the fabrication time was too long for many industrial applications, and consequently the idea of a spray-LBL method, where solutions were sprayed directly onto substrates, was conceived.[10] Fabrication time was reported to be greatly shortened due to enhanced adsorption by the spray pressure. An automated spray LBL machine has been previously reported.[11] The original features of our apparatus are (1) real-time QCM sensing and (2) separate control of spray pressure, solution flow rate, and spray scanning pattern. The spray-LBL method is still an emerging field of research,[12−16] and mechanisms during spraying have yet to be investigated. Uninvestigated parameters include spray pressure, adsorption time, distance between spray nozzle and substrate, diameter of nozzle, size of droplet, etc. There are reports[18−20] of QCM techniques having been used to determine film mass, but not for real-time monitoring during the spray-LBL process.

In the current study, an automatic spray-LBL machine was fabricated and film reproducibility examined. *In situ* monitoring was realized using QCM techniques, and the optimization of film fabrication conditions was carried out. The spray-LBL method provided sufficient film quality for their application as optical thin films.

EXPERIMENTAL SECTION

Materials. For the low reflective index layer, poly(allylamine hydrochloride) (PAH) and poly(acrylic acid) (PAA) were used as the polycations and polyanions, respectively. For the high reflective index layer, poly(diallyldimethylammonium chloride) (PDDA) was used as the polycation, and titanium(IV) bis(ammonium lactato)dihydroxide (TALH) was prepared. All materials were purchased from Sigma-Aldrich and were used without further purification.

Fabrication of the Automatic Spray-LBL Machine. There are previous reports of an automatic spray-LBL machine.[20] We have fabricated an automatic machine which could uniformly spray on wide substrates. A schematic of our machine is shown in Figure 1.

Three pumps were incorporated for the rinsing of the cationic, anionic, and Milli-Q solutions, as it was necessary to independently

Received: January 6, 2011
Revised: March 15, 2011
Published: April 04, 2011

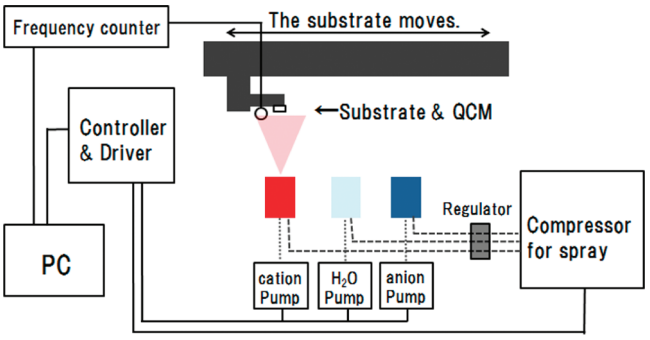

Figure 1. Automatic spray-LBL machine. Substrates and QCM were fixed on the stage, and all steps were computer controlled.

Table 1. Stage Times

	time (s)	
step	cation	anion
1. stable state	30	30
2. spraying	10	10
3. waiting state	10	10
4. rinsing state	10	10
5. drying state	10	10
	70	70
total	140	

change their flow rates. A regulator was used to control the spray pressure from a single compressor. Thus, spray pressure could be altered by changing flow quantities. The QCM electrode was positioned near to the substrate to ensure it was also coated at the same time. QCM frequency data were counted with a frequency counter and were output to a PC for analysis. This system provided us with the real-time increase in film mass. All operations such as repetition frequency and movement patterns were computer controlled. The distance from spray nozzle to substrate was fixed, and spray pressure was controlled at the proper value. A high volume compressor was utilized to maintain constant conditions and prevent pressure decrease during film fabrication.

Measurements. Film thickness was determined by ellipsometry measurements (ULVAC ESM-1A). Optical characterization of multilayer films was carried out using an ultraviolet−visible (UV−vis) spectrophotometer (Shimadzu UV mini-1240). Surface images were captured by field-emission scanning electron microscopy (FE-SEM; Hitachi S-4700) and atomic force microscopy (AFM; Nanoscope IIIa, Digital Instruments). Optical simulation software (DESIGN, TECWAVE) was used.

Film Preparation. *Substrate Preparation.* QCM substrates were placed in an ozone atmosphere under UV irradiation for 6 h to ensure hydrophilicity. Silicon wafers were also treated by UV irradiation for 2 h to form a hydrophilic surface and were used to investigate deposited film thickness and reflective index. UV irradiation removed any organic contamination present on the substrate. Glass slides were ultrasonically agitated in a KOH solution (1.0 wt %) of ultrapure water and ethanol (2:3 v/v) for 3 min and then twice rinsed with ultrapure water for 5 min. From this treatment, substrates were cleaned and negatively charged.

Solution Preparation. The concentrations of PAH, PAA, and PDDA solutions were all 0.01 mol/L, and that of the TALH solution was 2 g/100 mL. Solutions were stirred overnight. Their pH was adjusted by adding 0.1 mol/L NaOH or 0.1 mol/L HCl (PAH:3.5, PAA:3.5, PDDA:5.5, TALH:3.5). After pH adjustment, solutions were used within a few hours.[21−23]

Spray Conditions. Parameters were divided into fixed and variable parameters. The nozzle diameter was 1.2 mm, and droplet size was 10−100 μm. Solution and water flow rates were adjusted to 4.0 mL/min. The distance between substrate and spray nozzle was fixed to 15 cm, and the sprayed area was a circle of diameter ∼4 cm. Spray pressure and spray time were variable parameters. The pressure was measured nearby the spray nozzle during air flow and controlled at 0.025, 0.05, and 0.075 MPa. Times of each step were as given in Table 1.

RESULTS AND DISCUSSION

***In-Situ* Monitoring by QCM.** Adsorption characteristics of $(PAH/PAA)_n$ films were observed by QCM (Figure 2). Frequency data were displayed as the change of frequency from a stable state (*Y*-axis) relative to time (*X*-axis). The procedure could be divided into five steps: (1) stable state; (2) spraying state; (3) waiting state; (4) rinsing state; (5) drying state. These steps are also displayed in Figure 2.

Step 1: Stable State. The frequency changed little during the stable state. No water, spray pressure, or adsorption was present on the QCM surface, and the quartz crystal oscillated steadily. The average frequency during the first stable state was defined as the base frequency for subsequent stages.

Step 2: Spraying State (Solution). When solutions were sprayed, the QCM frequency rapidly decreased and there was significant noise. The frequency decreased because of the adsorption of water and other solutions. Pressure on the QCM surface induced significant noise so the spraying state was unsuitable for measuring the adsorbed mass increase.

Step 3: Waiting State. The frequency increased a small amount and the noise disappeared. As droplet presence was not constant, the waiting state was also unsuitable for estimating the quantity of adsorbed material.

Step 4: Rinsing State (Pure Water). The frequency during the rinsing state was similar to that at the spraying state, and frequency decreased and fell into disorder. Some surplus aggregation was removed, with only absorbed polymer bonded remaining on the quartz surface.

Step 5: Drying State. The QCM surface was then dried by blowing with air. The frequency rapidly increased as any remaining water was removed, and frequency recovered to near stable state values. Again the pressure on the QCM crystal caused significant noise, and it was not possible to estimate mass increase.

Frequency Change and Film Thickness. Ten cycles ware carried out, and a ten-bilayer film was fabricated on the QCM, silicon wafer, and glass slide. The film on the slide glass was flat and transparent. The film mass on the QCM crystal and the film thickness on the silicon wafer were measured and compared using ellipsometry.

As shown in Figure 3, the QCM frequency at the stable state linearly decreased because the frequency change was the same at every bilayer, and a stable state had occurred at every cycle. It shows the linear growth of film mass with increasing number of bilayers. At the end of ten cycles, the total frequency decrease was 760 Hz.

As shown in Figure 4, the silicon wafer film thickness was measured by ellipsometry, and film thickness increased linearly. After ten spray cycles the film thickness was about 17 nm. A film thickness increase of ∼1 nm was estimated from the 45 Hz

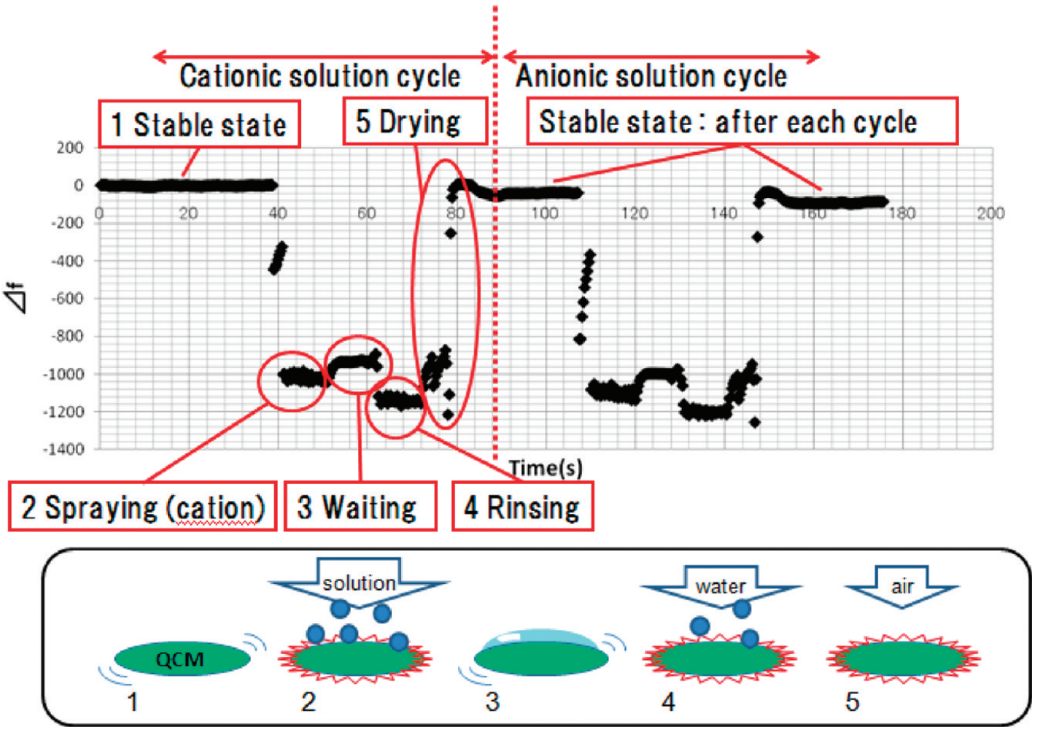

Figure 2. *In-situ* monitoring by QCM, showing one cycle for a (PAH/PAA) film. Five distinct stages were apparent: (1) stable state; (2) spraying state, (3) waiting state, (4) rinsing state, (5) drying state. Stage times are shown in Table 1.

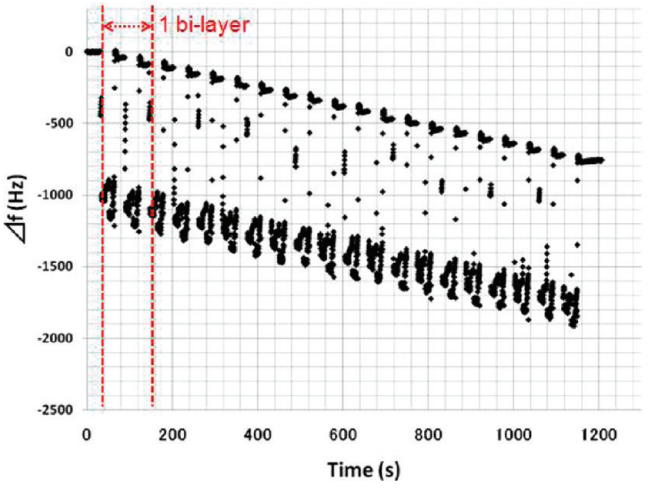

Figure 3. *In-situ* monitoring by QCM, showing ten cycles of (PAH/PAA) film being prepared. The spraying cycle was repeated using PAH and PAA, so stable states occurred 20 times.

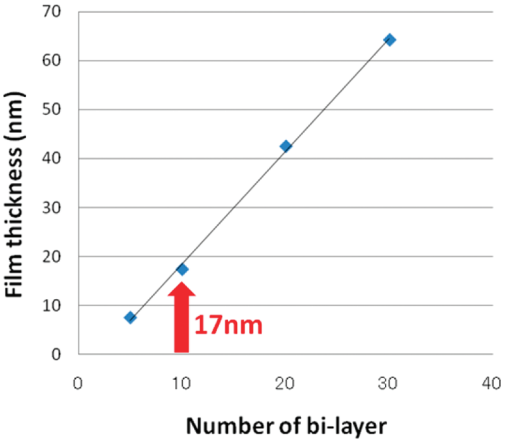

Figure 4. Film thickness measured by ellipsometry, with (PAH/PAA) films of 5, 10, 20, and 30 bilayers measured.

frequency decrease. In the absence of QCM, measuring film thickness precisely by ellipsometry required the drying of the silicon wafer film. To the best of our knowledge, there are no previous reports of the real-time monitoring by QCM. Using the QCM system, film thickness could be monitored in real time regardless of substrate type. Quantitative correlation of the frequency change on the QCM and substrate film thickness should first be investigated, and once this relationship is known, reproducible film growth data are always obtained. The high film reproducibility is a significant advantage for industrial applications. Optical thin films require precise and reproducible control of film thickness. As some time was required to stabilize the QCM, this procedure took a little longer than those reported elsewhere. To ensure a flat film and uniform thickness distribution, the spray nozzle was moved in parallel with scanning of the substrate. Thus, smaller samples could be prepared in less time. The improvement in reproducibility with using the automatic spray-LBL machine is a significant result and could accelerate the development of spray-LBL for optical applications.

Surface Structure (Compared with Dipping Method). To compare surface structures with those from the dipping method, we also fabricated (PAH/PAA) films using the conventional dipping method with the same PAH and PAA solutions (100 mL). Negatively charged glass substrates were immersed in cationic PAH solution for 5 min and then rinsed three times in

dx.doi.org/10.1021/ma200024w |*Macromolecules* 2011, 44, 2964–2969

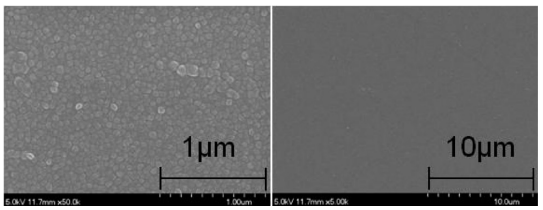

Figure 5. SEM images of the $(PAH/PAA)_{20}$ film fabricated by the dipping method: (a) ×50K and (b) ×5K.

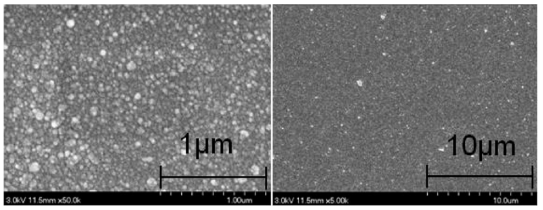

Figure 6. SEM images of the $(PAH/PAA)_{20}$ film fabricated by the automatic spraying method: (a) ×50K and (b) ×5K.

pure water for 1 min. The substrate, now positively charged by PAH, was then immersed in anionic PAA solution, and the same rinsing process was carried out. This cycle was repeated 20 times, and after drying by air blowing the final $(PAH/PAA)_{20}$ film was obtained. Images of the surfaces were captured by SEM and are shown in Figures 5 and 6. Figure 5 shows images from films fabricated by the conventional dipping method, from which aggregations of 300−1000 nm in size were apparent on the surface. The roughness was small and the surface flat and smooth. Figure 6 shows that films fabricated by spray-LBL were a little rougher than those from the dipping method, but aggregation size was similar. For optical thin film applications, surface roughness decreases film quality because it results in light scattering. Thus, films fabricated by spray-LBL were optically flat, so the machine is suitable to the fabrication of optical thin films.

Film Thickness and Spray Pressure. We also investigated the effect of spray pressure on film thickness. There are many reports of thin films fabricated by spray-LBL,[10−16] but none have studied the effect of spray pressure. Experimental conditions also appear to have resulted in difficulties reproducing spray conditions in some reports.[10] To maintain spray pressure without loss, a stable compressor such as the one employed in the current study was necessary. The spray-LBL process is significantly faster than the conventional dipping method, which has been attributed to spray pressure in the vertical direction promoting film growth.[12,13,15] A quantitative effect of spray pressure change should then be observed, in that film growth should become faster with increasing pressure. The effect of pressure during rinsing must also be considered. There also exists the potential for differences in reflective index or surface morphology. We examined the influence varying spray pressure (at 0.025, 0.05, and 0.075 MPa) on film characteristics (such as thickness), which was easily carried out with the automatic spray-LBL machine. Pressure was measured nearby the spray nozzle during air flow. Since the spray nozzle used in this study required a lot of air, the pressure measured was lower than that at the discharging point of the compressor. A nozzle requiring much air can produce numerous droplets, so the solution could be spread widely over substrate.

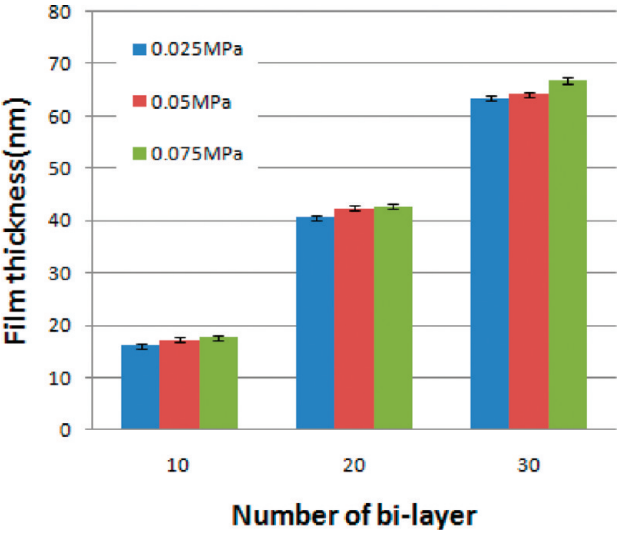

Figure 7. Comparison of (PAH/PAA) film growth at different pressures of 0.025, 0.05, and 0.075 MPa. Film thickness was measured by ellipsometry.

The 10-, 20-, and 30-bilayer films were first deposited on silicon wafers, and their thickness was then measured (Figure 7). For each of the three samples, film growth was slightly bigger when the spray pressure was stronger, so the effect of spray pressure was not pronounced. The error margin was within 0.5 nm, which was smaller than the thickness difference between samples. While the effect of the pressure was not linear, it was at least clear that film growth was promoted from increased pressure.

It was thought that spray pressure in the vertical direction promoted film growth and density. When the reflective index increased, film density at every bilayer became larger. It was necessary to maintain spray pressure and hold other conditions constant to retain film quality. For optical devices where film thickness and refractive index must be precisely controlled, precise pressure control was critical in maintaining film quality.

Antireflective Films. From QCM, SEM, and ellipsometry results, different film characteristics were revealed from different pressures, including film thickness, mass, reflective index, and surface morphology. We then tried to apply the spray-LBL method to an antireflective film (AR), which has a double construction.[28,30] AR films cause the interference with reflected light because the film possesses an optical film thickness of a quarterwave.[3−5] AR films are used in glasses and solar batteries, and since wavelength transmission can be used to generate electricity, AR films are useful for improving power generation efficiency. AR films can be created from a single layer which has a refractive index lower than glass,[29] but the effect becomes small as the wavelength narrows. AR effects are greatly improved when optical thin films accumulate the high refractive index film of the quarterwave between a low refractive index layer and the substrate. With precise design, the wavelength window of the reflection can be expanded or narrowed. In this study, we attempted to apply AR films to glasses. The material for the high reflective index layer was poly(diallyldimethylammonium chloride) (PDDA) as the polycation, and titanium(IV) bis(ammonium lactato)dihydroxide (TALH) was prepared.[24−27] We attempted to fabricate the film using the spray-LBL method with the same solutions and successfully fabricated the

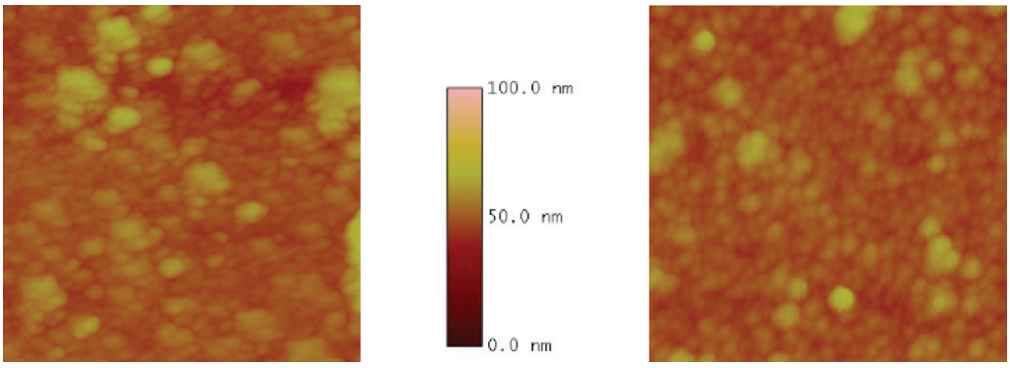

Figure 8. AFM images from a 1 μm square of a $(PAH/PAA)_{20}$ film fabricated by the automatic spraying method. (a) Spray 0.05 MPa, rms = 4.513 nm. (b) Spray 0.075 MPa, rms = 3.970 nm.

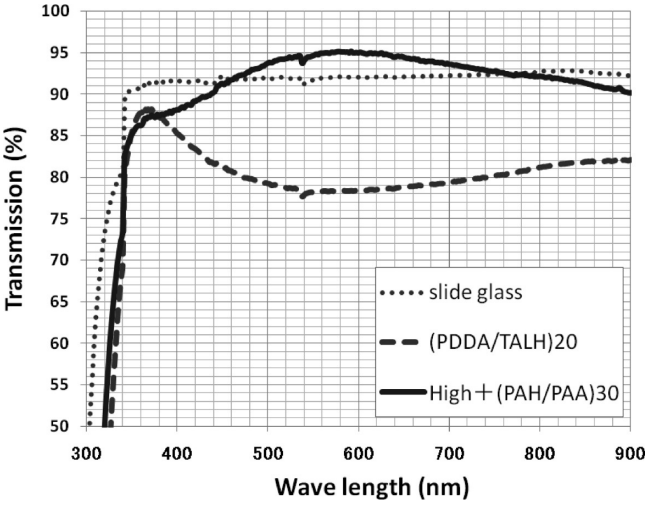

Figure 9. Optical characteristics of films measured by UV−vis spectrophotometry.

transparent high reflective index layer. Film construction aimed to prevent wavelengths of 550 nm, and a simulation was carried out by the software. Film thickness was calculated from the refractive index, and the film was continuously layered until the desired thickness was reached. The optimization of refractive index requires further investigation.

Two glass slides were first cleaned, and a hydrophilic surface formed by treatment with KOH. The (PDDA/TALH) film was then prepared on the glass slide. One slide was dried at room temperature to aid measurements, and its reflective index and film thickness were 1.84 and 79 nm, respectively. The second slide was used for fabricating the AR film. Prior to its surface drying completely, a low refractive index 30-bilayer (PAH/PAA) film was prepared. The reflective index and film thickness were 1.49 and 99 nm, respectively. Films were fabricated using identical spray-LBL conditions. Following drying of the films at room temperature for 6 h, they were transparent, and their reflected light was slightly purple due to interference. The reflection decreased and the antireflection effect was confirmed by a visual check. Figure 9 shows that transmission greatly decreased when only the high refractive index layer was present on the slide glass. This transmission decrease was due to an increase in reflection, since scattering was not observed and absorption characteristics were small. The reflection arose from the phase gap from interference in the high refractive index layer which had quarterwave film thickness. For the AR film on which the low reflective index layer had been prepared, Figure 9 shows that transmission at ~550 nm increased about 5% in comparison to that of the uncoated glass slide. At 450−700 nm, transmission was also higher than that for the bare glass slide.

CONCLUSIONS

We succeeded in the *in-situ* monitoring of LBL-film growth using QCM, during film deposition using the spray method. We controlled the film thickness at the nanoscale order accuracy using the newly developed spray-LBL machine. Differences in film characteristics between different spraying conditions were demonstrated. Higher film deposition speeds were observed with higher spray pressures. The connection with QCM frequency change and film thickness was confirmed from different spray pressures. We also succeeded in fabricating antireflection (AR) films. UV−vis data showed that visible light transmission was higher than that for bare glass slides. The fabrication of the automatic spray-LBL machine and real-time QCM measurement allows the control of film thickness and the fabrication of optical thin films.

AUTHOR INFORMATION

Corresponding Author

*E-mail: shiratori@appi.keio.ac.jp. Phone: +81-045-566-1602.

ACKNOWLEDGMENT

We thank Mr. Junichiro Abe for the fabrication of electric circuits for the automatic spray-LBL system. We also thank Prof. Michael Rubner of MIT for useful discussions.

REFERENCES

(1) Kim, J.; Fujita, S.; Shiratori, S. S. *Physicochem. Eng. Aspects* **2006**, *284*−*285*, 290–294.

(2) Maeda, R.; Iwamoto, T.; Shakutsui, M. *J. Photopolym. Sci. Technol.* **2009**, *22*, 525–528.

(3) Shimomura, H.; Cohen, R. E.; Rubner, M. F. *ACS Appl. Mater. Interfaces* **2010**, *2*, 813–820.

(4) Adam, J. N.; Rubner, M. F.; Cohen, R. E. *Langmuir* **2004**, *20*, 3304–3310.

(5) Srivastava, S. K.; Ojha, S. P. *Microwave Opt. Technol.* **2003**, *38*, 293–297.

(6) Druffel, T.; Mandzy, N.; Sunkara, M.; Grulke, E. *small* **2008**, *4*, 459–461.
(7) Walter, H.; Stuck, H. *Thin Solid Films* **2008**, *516*, 4656–4658.
(8) Mennig, M.; Oliveira, P. W.; Frantzen, A.; Schmidt, H. *Thin Solid Films* **1999**, *351*, 225–229.
(9) Fujimoto, K.; Kim, J.; Shiratori, S. S. *Jpn. J. Appl. Phys.* **2008**, *47*, 8644–8647.
(10) Schlenoff, B.; Joseph, B. S.; Stephan, T. D.; Tarek, F. *Langmuir* **2000**, *16*, 9968–9969.
(11) US Patent 6,896,926 B2, 2005; filed 2003.
(12) Izquierdo, A.; Ono, S. S.; Voegel, J. C.; Decher, G. *Langmuir* **2005**, *21*, 7558–7567.
(13) Félix, O.; Zheng, Z.; Cousin, F.; Decher, G. *C. R. Chim.* **2009**, *12*, 225–234.
(14) Krogman, K. C.; Zacharia, N. S.; Schroeder, S.; Hammond, P. T. *Langmuir* **2007**, *23*, 3137–3141.
(15) Porcel, H.; Izquierdo, A.; Ball, V.; Decher *Langmuir* **2005**, *21*, 800–802.
(16) Ono, S. S.; Decher, G. *Nano Lett.* **2006**, *6*, 592–598.
(17) Gamboa, D.; Morgan, A. P.; Ham, A. *Rev. Sci. Instrum.* **2010**, *81*, 036103.
(18) Ariga, K.; Hill, J. *Phys. Chem. Chem. Phys.* **2007**, *7*, 2969–2993.
(19) Shiratori, S. S.; Yamada, M. *Polym. Adv. Technol.* **2000**, *11*, 810–814.
(20) Okayama, Y.; Ito, T.; Shiratori, S. S. *Thin Solid Films* **2001**, *393*, 132–137.
(21) Kyung, K.; Fujimoto, K.; Shiratori, S. S. *Jpn. J. Appl. Phys.* **2010**, *49*, 045001.
(22) Yoo, D.; Shiratori, S. S.; Rubner, M. F. *Macromolecules* **1998**, *31*, 4309–4318.
(23) Shiratori, S. S.; Rubner, M. F. *Macromolecules* **2000**, *33*, 4213–4219.
(24) Shi, X.; Cassagneau, T.; Caruso, F. *Langmuir* **2002**, *18*, 904–910.
(25) Rouse, J. H.; Ferguson, G. S. *Adv. Mater.* **2002**, *14*, 151–154.
(26) Möckel, H.; Giersig, M.; Willig, F. *J. Mater. Chem.* **1999**, *9*, 3051–3056.
(27) Kim, J.; Fujita, S.; Shiratori, S. S. *Thin Solid Films* **2006**, *499*, 83–89.
(28) Chunder, A.; Etcheverry, K.; Wadsworth, S.; Glenn, D. *J. Soc. Inf. Display* **2009**, *17*, 389–395.
(29) Li, Y.; Liu, F.; Sun, J. *Chem. Commun.* **2009**, 2730–2732.
(30) Juan, I. L. *J. Opt. Soc. Am. A* **2001**, *18*, 1406–1414.